# A new design technique based on a suitable choice of rotor geometrical parameters to maximize torque and power factor in synchronous reluctance motors: Part I - Theory

Ivan Eduardo Chabu* Viviane Cristine Silva* José Roberto Cardoso* Silvio I. Nabeta* Albert Foggia**

*LMAG - Laboratório de Eletromagnetismo Aplicado / EPUSP - Escola Politécnica da Universidade de São Paulo
Av. Prof. Luciano Gualberto, Trav. 3 no. 158 ZIP: 05508-900 São Paulo SP - Brazil / E-mail: cardoso@pea.usp.br

**LEG - Laboratoire d'Electrotechnique de Grenoble URA CNRS 355 / BP 46 / F-38402 St. Martin d'Hères Cedex / France

*Abstract* – **The influence of rotor geometry of synchronous reluctance motors (SRM) on the $x_d/x_q$ ratio, on electromagnetic torque and on iron losses is studied . Both air-gap and rotor pole arc are taken into account as parameters. First, a new theoretical approach is developed which neglects saturation effects (Part I). In a companion paper (Part II), a complete finite-element analysis of a particular SRM is carried out, followed by a comparison with results obtained by tests performed in a prototype machine, which was constructed in order to validate the proposed methodology.**

## I - Introduction

The performance of a SRM is strongly affected by its rotor pole arc, as well as its air-gap length. The choice of these two parameters is limited by the motor efficiency, torque characteristics, power factor and iron losses. The most usual rotor geometry is illustrated in Fig. 1, which represents the case analyzed.

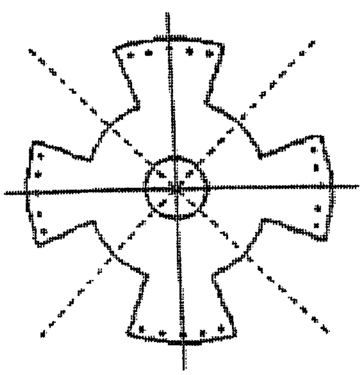

Fig. 1 Rotor of a SRM

## II - Power and torque characteristics

The phasor diagram allows evaluating of both active and reactive power of a SRM at steady state, as depicted in Fig. 2. By neglecting resistances and saturation effects, the active and reactive powers per phase in the case of a voltage-source feeding can be written as:

$$P_v = \frac{V^2}{2}\cdot\left(\frac{1}{x_q}-\frac{1}{x_d}\right)\cdot sin 2\delta, \qquad (1)$$

$$Q_v = V^2\cdot\left(\frac{sin^2\delta}{x_q}+\frac{cos^2\delta}{x_d}\right)\cdot sin 2\delta, \qquad (2)$$

and in the case of current-source feeding, they are written as:

$$P_i = \frac{I^2}{2}\cdot\left(x_d - x_q\right)\cdot sin 2\delta_i\ , \qquad (3)$$

$$Q_i = I^2\cdot\left(x_q \sin^2\delta_i + x_d\cos^2\delta_i\right). \qquad (4)$$

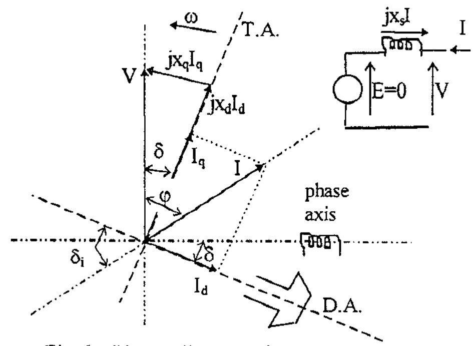


Fig. 2 - Phasor diagram of the SRM at steady state

As the speed is constant the torque characteristic is promptly obtained.

Fig. 3a and 3b present, respectively, the flux density in the air-gap for both direct and transverse axis in the case of a sinusoidal m.m.f. Thus, the flux per pole in both cases can be evaluated as follows:

$$\phi_p = \frac{DL}{p}\cdot\int_0^{\frac{\pi}{2}} \boldsymbol{B}(\theta)\,d\theta, \qquad (5)$$

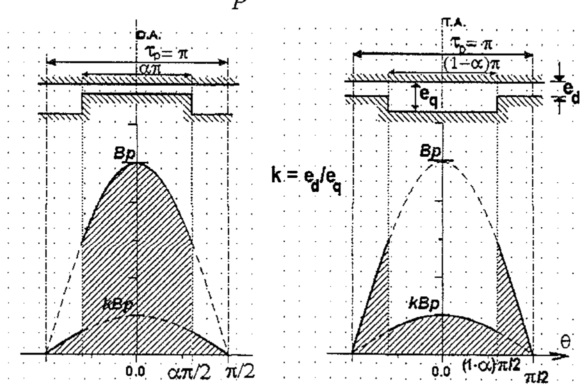


Fig. 3 - Flux density distribution: a) direct axis; b) transverse axis

0-7803-3946-0/97/$10.00 © 1997 IEEE TB1-5.1

Solving (5) for direct and transverse axis yields:

$$\phi_{p_d} = \frac{D \cdot L \cdot B_p}{p} \cdot f_d \,, \quad (6) \qquad \phi_{p_q} = \frac{D \cdot L \cdot B_p}{p} \cdot f_q \,, \quad (7)$$

with the factors $f_d$ and $f_q$ given by:

$$f_d = k + (1-k)\cdot sin\frac{\alpha\pi}{2}\,, \; (8) \qquad f_q = 1-(1-k)\cdot cos\frac{\alpha\pi}{2}\,, \; (9)$$

For both axis the flux per pole can be obtained from:

$$\phi_p = F_p \cdot P(\alpha,k) = \frac{B_p}{\mu_0}\cdot e_\alpha \cdot P(\alpha,k)\,, \qquad (10)$$

with $e_\alpha = k_g . e_d$ , which stands for the equivalent air-gap, whereas the permeance $P(\alpha,k)$ is given by:

$$P(\alpha,k) = \frac{\mu_0 \cdot D \cdot L}{p \cdot k_g \cdot e_d}\cdot f(\alpha,k)\,. \qquad (11)$$

The factor $f(\alpha,k)$ can be either $f_d$ for the direct axis (eq. 8) or $f_q$ for the transverse axis (eq. 9).

The m.m.f. per pole can be obtained by writing:

$$N_f \cdot \phi_P = 2p \cdot L_p \cdot I \cdot \sqrt{2}\,, \qquad (12)$$

yielding:

$$F_p = \frac{m\cdot\sqrt{2}}{\pi \cdot p}\cdot N_f \cdot I\,, \qquad (13)$$

Equations (10) to (13) lead to the following expression for the synchronous reactance per phase:

$$x_f = 2\pi f \cdot 2p \cdot L_p = A \cdot f(\alpha,k)\,, \qquad (14)$$

which equals to:

$$x_d = A f_d \quad \text{or} \quad x_q = A f_q \qquad (15)$$

depending of the value of $f(\alpha,k)$ ($f_d$ or $f_q$), and with $A$ given by:

$$A = \frac{2 f m \mu_0 D L N_f^2}{k_g e_d p^2}\,, \qquad (16)$$

Fig. 4 presents a graphic plotted with the variation of the $x_d/x_q$ ratio with respect to the pole arc length, using $k$ as a parameter.

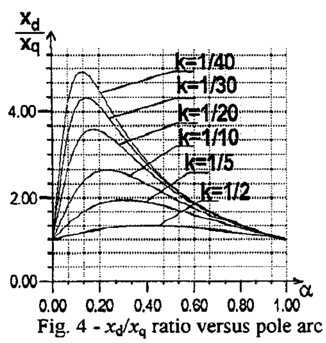


Fig. 4 - $x_d/x_q$ ratio versus pole arc

The torque characteristic is obtained from (1), (3) and (16) in the two following conditions: with voltage-source feeding and with current-source feeding, i.e.:

$$C_v = \frac{mV^2}{2\omega_s A}\cdot sin 2\delta \cdot f_v\,; \qquad (17)$$

$$C_i = \frac{m I^2 A}{2\omega_s}\cdot sin 2\delta_i \cdot f_i\,; \qquad (18)$$

The quantities $f_v$ and $f_i$ depend on the rotor geometry (see Fig. 5) and are called "torque factors". They are given by:

$$f_v = \frac{1}{f_q} - \frac{1}{f_d}\,, \quad (19) \qquad f_i = f_d - f_q\,. \qquad (20)$$

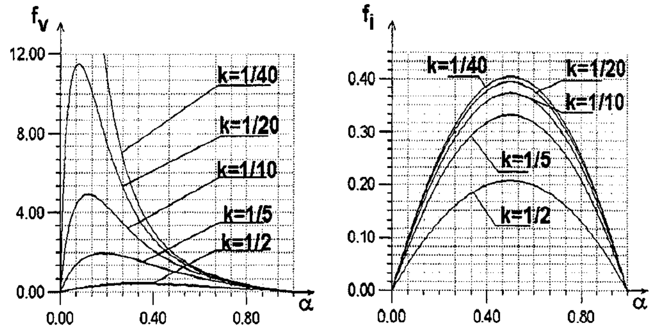


Fig. 5 - Torque factors vs. pole arc

The power factor also depends on rotor geometry (see Fig. 6) and in the cases of voltage-source and current-source feeding is given by:

$$cos\varphi_v = \frac{(x_d/x_q - 1)\cdot \sin 2\delta}{\sqrt{\left\{(x_d/x_q-1)^2 \cdot \sin^2 2\delta + 4\cdot\left[(1-x_d/x_q)\cdot\sin^2\delta - 1\right]^2\right\}}}\,, \quad (21)$$

$$cos\varphi_i = \frac{(x_d/x_q - 1)\cdot \sin 2\delta_i}{\sqrt{\left[(x_d/x_q-1)^2 \cdot \sin^2 2\delta_i + 4\cdot\left(\sin^2\delta_i + x_d/x_q \cdot \cos^2\delta_i\right)^2\right]}}\,. \quad (22)$$

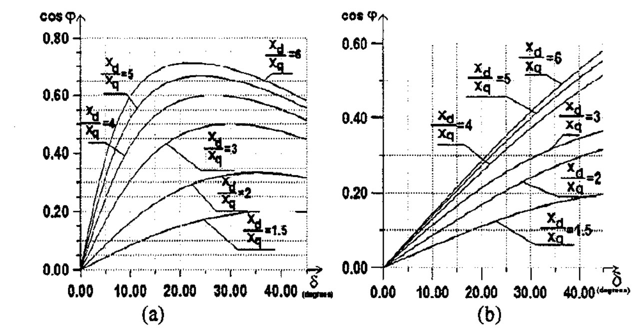


Fig. 6 - Power factor vs. δ (see Fig. 2): a) voltage source; b) current source.

## III - DESIGN ASPECTS

The design procedure of a SRM is conducted so as to select the rotor geometry that maximizes both torque and power factor, depending on the nature of the source: voltage or current feeding.

In the case of a voltage source, the pole arc that maximizes those quantities should be as shown in Fig. 5. However, the choice of the air-gap length is limited by mechanical constraints such as peripheral speed, tolerance, etc.

Typical dimensions for a SRM require a value of $k$ varying from 1/20 to 1/50. In this case the optimal pole arc should be less than 0.2.

In the case of a current-source feeding the optimal pole arc that maximizes both torque and power factor should be about 0.5.

The main electrical constraints that should be considered in the choice of the pole-arc and air-gap lengths of a SRM are the iron losses, since, in the presence of a short pole arc, the flux densities in the stator teeth can be very high.

### IV - Iron Losses

In order to evaluate the increase in the iron losses at no-load, let us take the following ratio:

$$\frac{P_i}{P_{i_0}} = \frac{B^2}{B_0^2} = \beta, \qquad (23)$$

with $B$ and $B_0$ being, respectively, the r.m.s. flux density in the air-gap corresponding to the direct axis and the r.m.s. flux density in the air-gap for a non-salient-pole machine ($\alpha = \pi$). The flux per pole is the same in both cases so as to compare the iron losses.

The r.m.s. flux density in the direct axis is written as:

$$B = B_p \cdot \sqrt{\left\{\frac{k^2}{2} + \frac{\left(1-k^2\right)}{2} \cdot \left[\alpha + \frac{sin\left(1-\alpha\right)\cdot\pi}{\pi}\right]\right\}} \;, \qquad (24)$$

and the r.m.s. flux density in a non-salient-pole machine is given by:

$$B_0 = B_{p_0} / \sqrt{2}\,. \qquad (25)$$

By evaluating $B_{p0}$ in order to obtain the same value of flux per pole in both machines, it can be shown that:

$$\beta = \frac{k^2 + \left(1-k^2\right)\cdot\left[\alpha + \frac{sin\,\pi\cdot\left(1-\alpha\right)}{\pi}\right]}{\left[k + \left(1-k\right)\cdot sin\frac{\alpha\pi}{2}\right]^2}\,. \qquad (26)$$

Fig. 7 illustrates the variation of β with respect to the pole-arc α.

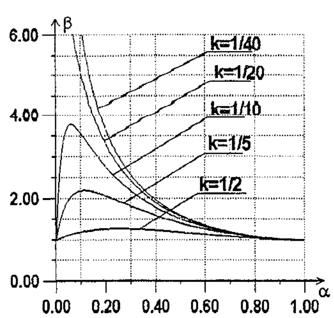


Fig. 7 - Factor β representing the increase in the iron losses.

By comparing the iron losses in salient- and non-salient-pole machines for $\alpha \sim 0.2$ and $k = 1/40$, it can be seen that stator teeth iron losses can increase 4 to 6 times. Supposing that iron losses in the yoke are equal to the losses in the teeth in the non-salient pole machine, the global iron losses of the salient-pole machine can be twice or 3 times as high as those of a non-salient-pole machine.

### V - Conclusions

New design procedures have been proposed so as to maximize both torque and power factor characteristics of SRMs, as well as to minimize iron losses. They are based on a theoretical analysis of the influence of rotor geometrical parameters (e.g. air-gap and pole arc) on those quantities. This influence (relating the electrical and mechanical quantities with geometrical parameters) is presented both in algebraic and graphical representation, thereby enabling the optimal choice of the relevant geometrical parameters.

The validation and efficiency of the results obtained are presented in a companion paper (Part II - Finite-element simulation versus measurements) in two different ways: first, they are compared with numerically simulated values provided by a 2D finite-element package, and second, they are compared against measurements performed in a prototype machine.

### Acknowledgments

The authors are very grateful to *USP/COFECUB* - a Brazilian/French Cooperation - for their financial support. The authors also acknowledge *EQUACIONAL LTDA.* for providing the experimental data of the prototype machine, and LEG - *Laboratoire d'Electrotechnique de Grenoble* (France) - for authorizing the utilization of FLUX2D package.

### List of Symbols

| | | |
|---|---|---|
| $\alpha$ | : | ratio of pole arc and pole pitch |
| $\delta$, $\delta_i$ | : | see Fig.2 |
| $k$, $k_g$ | : | ratio of air-gaps and Carter factor |
| $B_p$ | : | peak value of the spatial flux density distribution |
| $F_p$ | : | peak value of the 1st harmonic m.m.f. per pole |
| $L_p$ | : | inductance per pole |
| $N_f$ | : | number of turns per phase |
| $D$, $L$ | : | stator internal diameter and length of the SRM |
| $m$, $p$ | : | number of phases and pole pairs |

### References

[1] I.E. Chabu, J.R. Cardoso, "Projeto de motores elétricos pelo método dos elementos finitos: comparação analítica/numérica/experimental", Proceedings of II SIMEAR - International Seminar in Electrical Machines and Drives, 07-09th. May 1991, São Paulo, pp. 83-99 (in portuguese).

[2] M.G. Say, "Alternating current machines", Longman Scientific & Technical, 5th edition

[3] J.R. Hendershot Jr., T. Miller, "Design of brushless permanent-magnet motors", Magna Physics Pub. & Clarendon Press Oxford Science Pub., 1994.

[4] T. Matsuo, T.A. Lipo, " Rotor design optimization of synchronous reluctance machine", IEEE Transaction on Energy Conversion, Vol. 9, No. 2, June 1994, pp. 359-365.